

# VIBRATING WIRE SENSORS FOR BEAM INSTRUMENTATION

Arutunian, S.G.  
Yerevan Physics Institute, Armenia

## Abstract

Thermal sensors based on the vibrating wire principle are distinguished by high accuracy and stability. An important advantage of these sensors is that they produce a frequency signal that can be transferred large distances without disturbance. Original vibrating wire sensors and monitors for the measurement of beam transversal characteristics of charged-particle and photon beams are described. By means of these devices, measurements of an electron beam in the Yerevan synchrotron, a proton beam at PETRA (DESY), and a hard x-ray undulator beam at the APS (ANL) have been performed.

## INTRODUCTION

The operating principle of Vibrating Wire Sensors (VWS) or Vibrating Wire Monitors (VWM) is based on the measurement of the change in the frequency of a vibrating wire, which is stretched on a support, depending on the physical parameters of the wire and environment in which oscillations take place. Today the area of application of this technique is expanding and the number of vibrating wire-based instruments has increased. Strain, displacement, piezometric level, pressure, angle and moment of rotation, viscosity of the media, and ultralow thermometry under 1 K are measured by VWS [1-7]. An interesting vibrating wire field-measuring technique has been developed for determination of magnetic center of units in accelerators (see, e.g., [8-10]).

The important advantages of properly constructed vibrating wire sensors are inherent long-term stability, high precision and resolution, good reproducibility and small hysteresis. Another advantage is that the frequency signal is imperturbable and can be transmitted over long cables with no loss or degradation of the signal. The reliability of the sensors becomes the overriding feature in the selection of a technology. It is also important to ascertain a low drift and minimum change in sensitivity. An important parameter of vibrating wire-based sensors is their ability to operate in hard conditions (high operational power and temperature cycling, thermal shock, thermal storage, autoclaving, fluid immersion, mechanical shock, electromagnetic and electrostatic environments [11]).

We take an electromechanical resonator with a metallic vibrating wire excited by the interaction of a current with a permanent magnetic field as a basis for the VWS of electron and proton beams. In this paper we discuss an application of such resonators for precise profile measurement of particle and photon beams. The interaction of the beam with the wire mainly causes heating of the wire. Thus we expect that the frequency of

natural oscillations of the wire will provide information about its temperature. The thermal method of measurement also allows registering neutron flux.

## MAIN CHARACTERISTICS

The operating principle of vibrating wire sensors is measurement of the change in the frequency of a vibrating wire, which is stretched on a support, depending on the physical parameters of the wire and the environment in which oscillations take place. A detailed description of the vibrating wires sensors can be found in our publications (see [12] and cited references). Below we present a short description of the VWS and some aspects not discussed in previous publications.

### Sensor main components

In Fig. 1 the sensor main components are presented. Wire (1) ends are pressed in the clips (2) and pass through the magnet field system (samarium-cobalt permanent magnets and magnet poles (3) and (4)). The magnet provides field strength on the order of 10 kG in the gap. Clips are fixed on the sensor support structure (5). Sensor is fastened on the scan feed arm by details (6) and (7).

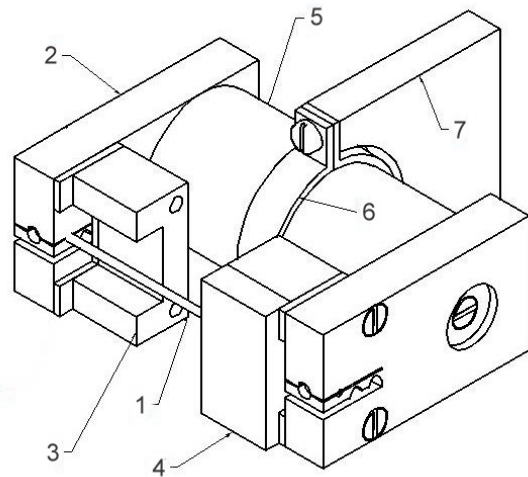


Fig. 1: Vibrating wire sensor main view.

By use of a simple positive feedback circuit, the magnetic system excites the second harmonic of the wire's natural oscillation frequency while keeping the middle of the wire exposed for detection of beam heating.

### Wire oscillation excitation

Wire oscillations arise as a result of the interaction between the oscillating current through the wire and the applied magnetic field. When the oscillating current passes through the wire, the Lorentz force shifts the wire in the transverse direction proportionally to the magnitude of the magnetic field and the peak current. The induced voltage is proportional to the time derivative of the current, which from the electrical viewpoint is equivalent to an inductance. The electrical equivalent of the wire can therefore be described as a series combination of a resistance and an inductance (see, e.g., [13]). Thus excitation of mechanical oscillations in the wire is possible because the wire acts like a tuned circuit when placed in an amplifier feedback arrangement. When the wire is connected to an amplifier circuit, a small amount of energy is fed back to the wire, which causes it to vibrate. This is similar to the excitation of electromechanical oscillations in quartz resonators (see, e.g., [14]). The frequency measurement is accomplished by counting the short impulses of the quartz generator inside a few periods of measured oscillations.

### Wire under beam irradiation

The interaction of the beam with the wire mainly causes heating of the wire due to the energy loss of the particles in the wire. In case of permanent thermal flux falling on the wire, the equilibrium temperature profile along the wire is determined by the balance between the heat deposited on the wire and heat dissipation occurring in three ways: thermal conductivity along the wire, heat radiation and convective heatsink (in gas media) [15]. A change in wire mean temperature results in a change of wire strain, which is registered by measurement of the wire's natural oscillation frequency. The second harmonic frequency of natural oscillations (if wire elasticity is neglected) is written as

$$F = 1/l \cdot \sqrt{\sigma/\rho}, \quad (1)$$

where  $\rho$  is the density of wire material,  $\sigma$  is the stress of the wire with ends pressed in clips on the distance  $l$ . Change of this value on  $\Delta l$  leads to a change in wire stress  $\Delta\sigma = E \Delta l/l$  (where  $E$  is the modulus of wire elasticity). As a result, the relative change of frequency is

$$\Delta F / F = E/2\sigma \cdot \Delta l/l. \quad (2)$$

The same effect arises if instead the wire is overheated by an amount  $\Delta T$ . This can happen if a localized heat flux falls on the wire (e.g., a beam of the particles or photons). Then  $\Delta l/l = -\alpha_s T$ , where  $\alpha_s$  is the coefficient of thermal expansion of the wire, and Eqn. (2) is rewritten:

$$\Delta F / F = -E/2\sigma \cdot \alpha_s \Delta T \quad (3)$$

This equation includes the large dimensionless factor  $E/2\sigma$ , which determines the high sensitivity of wire natural oscillation frequency to its heating. Thus for Sstainless steel  $E$  is of order 200 GPa, whereas  $\sigma$  is much less than tensile strength: of order of 500-800 MPa. If we measure the frequency with an accuracy of about 0.01 Hz, (this is the frequency measurement resolution at 1 s sampling) the corresponding temperature resolution is less than 0.001 K.

### Frequencies resonant capture

So-called frequencies resonant capture [16] can be obtained in coupled mechanical oscillators with several wires. This phenomenon can happen for multiwire VWS if resonant frequencies are very close. This effect is stipulated by common clips and support that form a mechanical coupling between wires.

Shown in Fig. 2 are data when resonant capture was aroused for two- wire VWS. Each frequency is measured by a separate electronic unit with a measurement gate of 30 s, which allows resolution down to 1 mHz. During the experiment the environmental temperature was also measured. Splitting of the frequencies occurred at 23:31 after which both frequencies moved to new values. This data allows for an estimation of the two measurement channel's accuracy by calculating the difference between the captured frequencies (see Fig. 3). One can see from the data that the frequency measurement channel accuracy is about 1 mHz.

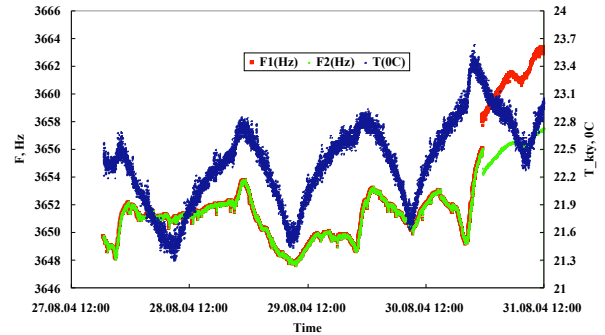


Fig. 2: Frequencies capture phenomenon for two wire resonator.

### Multiwire sensor wire thermal air coupling

If a multiwire sensor is used in the air a thermal coupling between sensor wires occurs. In addition to the external heat source (measured beam), the wire also reacts to temperature changes in neighboring wires. In this case, one must recover the necessary information about contributions of external sources from wire integral overheating.

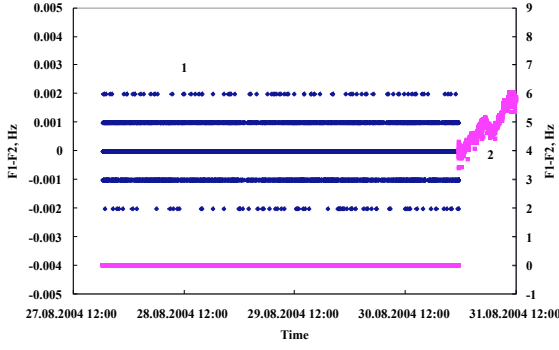


Fig. 3: Two oscillator frequencies difference at resonant capture. The same values are presented in two scales (1 – at left axis, 2 – at right).

For effect estimation we performed an experiment with a five-wire sensor when the external source was modeled by DC current through the given wire. In Table 1 the wire overheatings are presented. Each row corresponds to a current of about 10 mA passing through the subsequent wire. The offset between the wires was 0.5 mm (the second wire by technical reasons was omitted from measurements).

Table 1

wire 1	wire 2	wire 3	wire 4	wire 5
0.255	-	0.052	0.031	0.019
-	-	-	-	-
0.050	-	0.283	0.099	0.051
0.029	-	0.101	0.265	0.090
0.019	-	0.051	0.090	0.247

With good accuracy, (about 0.001 K) the values in the table are symmetric across the diagonal of the matrix.

With respect to a linear heat transfer model, the heat coupling between the wires is determined by the following equations:

$$\begin{aligned}
 Q_1 &= \alpha_{11}T_1 + \alpha_{12}(T_1 - T_2) + \alpha_{13}(T_1 - T_3) + \alpha_{14}(T_1 - T_4) + \alpha_{15}(T_1 - T_5), \\
 Q_2 &= \alpha_{12}(T_2 - T_1) + \alpha_{22}T_2 + \alpha_{23}(T_2 - T_3) + \alpha_{24}(T_2 - T_4) + \alpha_{25}(T_2 - T_5), \\
 Q_3 &= \alpha_{13}(T_3 - T_1) + \alpha_{23}(T_3 - T_2) + \alpha_{33}T_3 + \alpha_{34}(T_3 - T_4) + \alpha_{35}(T_3 - T_5), \\
 Q_4 &= \alpha_{14}(T_4 - T_1) + \alpha_{24}(T_4 - T_2) + \alpha_{34}(T_4 - T_3) + \alpha_{44}T_4 + \alpha_{45}(T_4 - T_5), \\
 Q_5 &= \alpha_{15}(T_5 - T_1) + \alpha_{25}(T_5 - T_2) + \alpha_{35}(T_5 - T_3) + \alpha_{45}(T_5 - T_4) + \alpha_{55}T_5.
 \end{aligned} \quad (4)$$

Here  $T_i$  are the wire overheatings relative to the environmental temperature, and  $Q_i$  is the power dissipated on the wire with index  $i$ . The right-hand sides of (4) define heat transfers with the environment (diagonal terms) and with the other wires. The coefficients  $\alpha_{ij}$  can be obtained by special experiments, however it is possible to determine them by scan data processing using the statement that the unknown beam distribution is the same for all wires (see below).

The problem also can be solved in a fashion similar to constant-temperature anemometry (see, e.g., [17]). By use of additional DC currents, frequencies can be stabilized at some level and in case of wire overheating by another source can be held at the same value by a corresponding decrease in DC current. The value of decrease is characteristic of the unknown source.

### Frequency dependence on environmental temperature

The wire oscillation frequency depends also on the environmental temperature. To minimize this dependence in our VWS, we used a compensation principle by choosing the coefficients of thermal expansion of the wire and support structure materials to be close to each other. For example, in the VWM005 the same grade of stainless steel was chosen both for the wires and the support. As a result, the dependence of frequencies upon environmental temperature variation decreases relative to characteristic value 40.2 Hz/K at frequency 4200 Hz for single wire (see Table 2). It is more convenient to compare the linear dependence of frequency squared on temperature; see equation (1). Multiple thermocycling of the five-wire sensor in the temperature range 30–70° C gives the values presented in Table 2. All values are much smaller than  $-3.38 \times 10^5$  Hz<sup>2</sup>/K for a single wire, but differ significantly from each other.

Table 2

	1	2	3	4	5
$dF^2/dT, 1000 \times \text{Hz}^2/\text{K}$	-5.5	-8.7	-7.4	-7.3	-8.3

Since all wires are made from the same coil of wire and are stretched on the same support, it follows that this difference is caused by the clips (plates of ceramics pressed by special elastic elements of sensor support). It seems that equal clamping of the wire ends will reduce the observed difference.

## BEAM INSTRUMENTATION

The high sensitivity of the VWS to wire temperature variation makes it well-suited to a wide range of accelerator diagnostic applications. Vibrating wire sensors have been applied to measurements of electron, proton and ion beams. VWS can be used for photon beam monitoring with very wide spectral range from deep infrared to hundreds of keV. Weak laser beams were successfully measured with VWS. First experiments have been performed for monitoring hard x-ray beams, both in vacuum and in air.

### Technical characteristics

The main parameters of oscillators with wires from stainless steel and tungsten are presented in Table 3.

Technical characteristics of 5-wire VWS in case of use in air are as follows: resolution of frequency measurement of each wire is 0.01 Hz, short time accuracy measurement (1 hour) is  $\pm 0.01$  Hz and accuracy in 24-hour interval is  $\pm 0.04$  Hz. Response time is 0.26 s. These values correspond to wire mean temperature resolution of 0.00025 K and short- and long-time accuracy  $\pm 0.00025$  K and  $\pm 0.001$  K. By such device it is possible to measure deposited on the wire power as small as  $\pm 1 \mu\text{W}$  in short-time mode and  $\pm 4 \mu\text{W}$  in long-time mode. The nonlinearity of the pickup in its operational range 0-100 mW is 0.01 %.

Table 3

Material, conditions	A316 Vacuum	A316 Air	Tungsten Vacuum	Tungsten Air
$\Delta T_{\text{mean}}/\Delta Q$ , K/mW	19.4	0.23	3.0	0.23
$\Delta F/\Delta T_{\text{mean}}$ , Hz/K at 4200 Hz	-40.2	-40.2	-8.8	-8.8
$\Delta F/\Delta Q$ , Hz/mW	-779.6	-9.3	-26.4	-2.0
response time, s	20.2	0.26	1.8	0.15

### Electron beam

The first scanning experiments on a charged beam were done on an electron beam at the Injector of Yerevan Synchrotron with an average current of about 10 nA (after collimation) and an electron energy of 50 MeV [19].

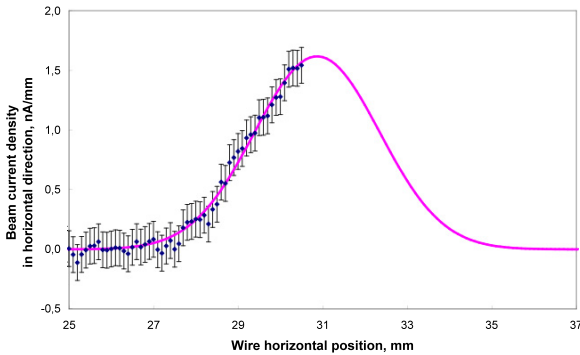


Fig. 4: Weak electron beam scan.

In Fig. 4 the result of the reconstruction of the beam profile for the first half-distance scan is shown. On the vertical axis the beam current density in the horizontal direction is presented. The solid line represents the profile of the beam approximated by the mean square method of a Gaussian function with a standard deviation of  $\sigma_x = 1.48$  mm and a beam position at 30.87 mm.

### Proton beam

A series of experiments with the VWS were done on a proton beam in the accelerator PETRA at DESY [12, 20-22]. The proton beam consisted of 10 bunches with an initial mean current of about 15 mA and an energy of 15 GeV. The transversal beam sizes were  $\sigma_x = 6$  mm,  $\sigma_z = 5$  mm. A system of two scintillator-photomultiplier pickups was installed additionally to measure particles scattered on the wire. The park position of the wire was located at 40 mm ( $6.7\sigma_x$ ) from the center of the vacuum chamber on the outside of the accelerator ring. The scanner was driven by a stepping motor toward the vacuum chamber center. A system of adjustable beam bumps allowed control the position of the beam inside the vacuum chamber at the scanner location.

An example of a beam scan is shown in Fig. 5. The signal from the VWS sensor changed from the beginning of the movement, while the signals from scintillators started to increase only at a distance of 13 mm from the VWS park position.

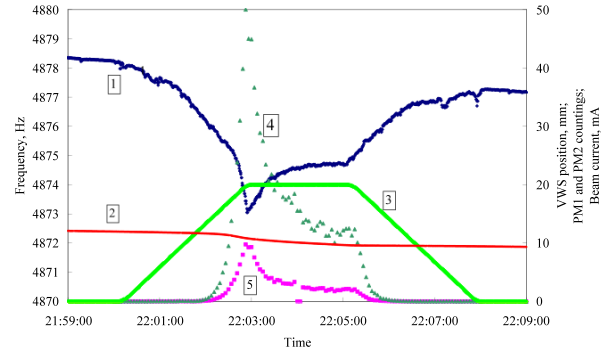


Fig. 5. Proton beam scan: 1, frequency signal; 2, proton beam current; 3, scan depth; 5 and 6, photomultipliers response.

The whole scan range was 20 mm. During the experiment (20 min) the proton beam current decreased from 12 mA to 9.5 mA. Shown in Fig. 5 are data collected at a 1 Hz sample rate during a scan.

### Ion beam

The vibrating wire scanner was also tested on an ion beam of the energy-mass analyzer EMAL-2 [23, 24]. Approximately 16 pA of beam current interacted with the wire and a frequency decrement of about 0.15 Hz was measured. The interest to continue ion beam profiling by the VWS is stimulated by the fact that the vibrating wire scanning method is based on thermal action of the beam and accumulates effect from both charged and neutral particles. By this method the effect of electrical neutralization of the ion beam by electron clouds can be overcome.

### Laser beam

A laser beam was scanned in air by a vibrating wire sensor with two wires located at distance 1 mm from each other [25-27]. A semiconductor laser of about 1 mW power was used as a photon source. A typical scan is presented in Fig. 6. The laser beam was scanned at a speed of 66  $\mu\text{m/s}$  forwards and backwards.

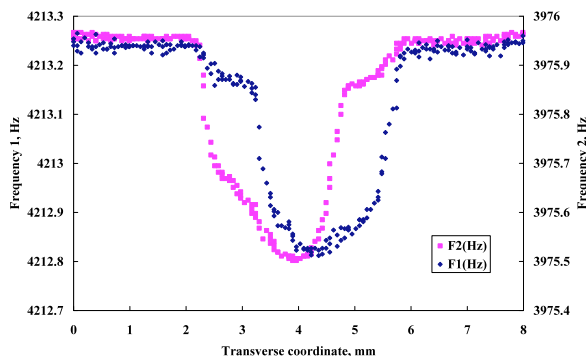


Fig. 6: Laser beam scan by two wire VWS.

Here we see the effect mentioned above of wire thermal coupling resulting in profile asymmetry.

### Hard x-ray beam monitoring in vacuum

Hard x-ray flux measurements with a vibrating wire monitor with two wires were conducted at APS [28]. The insertion device used was a standard APS undulator A.

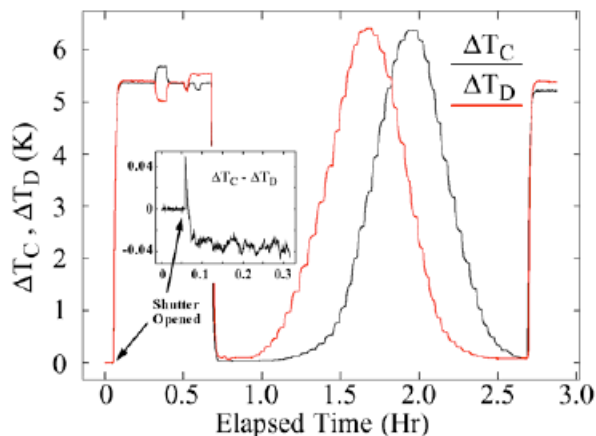


Fig. 7: Data collected during photon beam vertical angle scan.

A two-wire vibrating wire monitor was installed in a vacuum test chamber of beamline 19-ID. The initial frequencies were determined with the shutter closed at the start of the scan. Using these values, the temperature changes  $\Delta T_C$  and  $\Delta T_D$  were determined using equation (3), and these values are plotted in Fig. 7. The beam was steered downward by 100 microradians, and then steered in 5 microradian steps. A magnified view of the difference  $\Delta T_C - \Delta T_D$  is shown in the inset of Fig. 6.

With the shutter closed, the fluctuations fall in the range  $\pm 0.001\text{K}$ , while after opening the shutter with the beam approximately centered, the fluctuations are significantly larger, most likely the result of real beam motion. At the detector location, this  $\pm 0.001\text{K}$  translates into a noise floor near 0.5 microns. Considering the 52 meter distance from the source, this translates into less than 10 nanoradians angular resolution, which is quite remarkable.

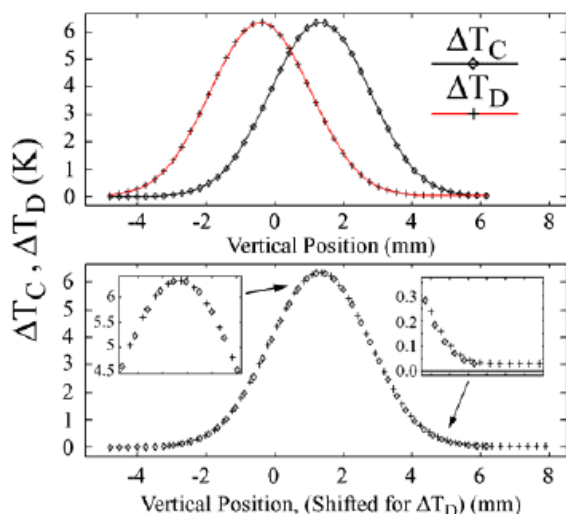


Fig. 8: VWM data corrected for thermal drift and beam current decay. The two data sets are offset in the lower panel for direct comparison.

Results of the scan after some data processing are shown in Fig. 8 (each of the 5-microradian step positions were fit to an exponential and thermal drift was subtracted). The plot of  $\Delta T_D$  was shifted by 1.730 mm in the lower plot, determined from the difference in centroid positions from the Gaussian fits. The wire separation measured later with a microscope was  $1.717 \pm 0.001$  mm. Because it was in vacuum, the VWM time constant was about 31 s (compared with calculated response time of 20 s from Table 3).

### Hard x-ray beam monitoring in air

Taking into account the extreme sensitivity of the vibrating wire sensors G. Decker suggested [28] placing the VWS outside of vacuum to detect only very hard x-rays that penetrate the vacuum chamber at selected locations (see also [29]). The addition of convective cooling reduces the response time substantially albeit with reduced sensitivity.

The VWM005 was mounted on the outboard side of a bending-magnet synchrotron radiation terminating flange in sector 37 at the APS storage ring, at a distance of about 7 m from radiation source. The synchrotron radiation power accepted in the horizontal angle corresponding to the VWM005 aperture (about 8 mm) is 99.1 W (at 100 mA beam current). Using spectral parameters for photon beam attenuation in Cu (material of flange) and stainless

steel (material of wire), one can calculate the spectral distribution of synchrotron radiation transmitted through the flange and deposited into the wire (see Fig. 9). The synchrotron radiation power after attenuation by 6 mm copper is 420 mW, while power dissipated into the wire is 1.13 mW. One can see from the list of the VWM005 parameters that this value is sufficient for registration by this sensor.

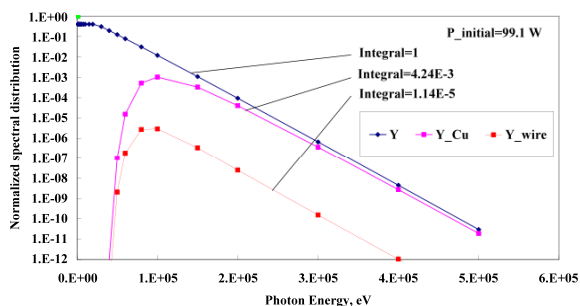


Fig. 9: Normalized spectral distribution of initial synchrotron radiation (Y), passed through the Cu flange (Y\_Cu) and deposited into the wire (Y\_wire).

In Fig. 10 we present the overheating data from the five-wire VWM when the electron beam angle was scanned vertically through a range of 300 microradians with 125 steps (for details see [30]). Profile asymmetries arise from the above-mentioned wire thermal coupling effect and some wire misalignment issues relative to the sensor housing.

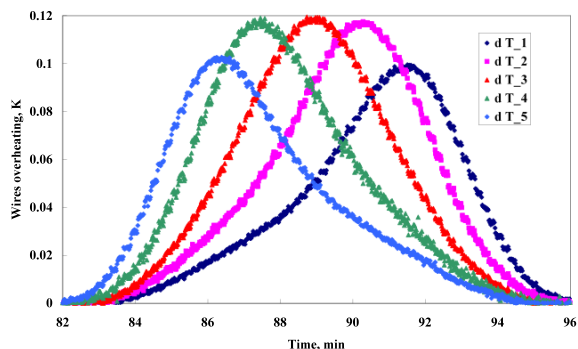


Fig. 10: APS vertical bending magnet angle scan results showing wire overheating temperatures.

Using a statistical data treatment, the heat coupling coefficients were found and accordingly (4) the profiles of the source were recovered (see Fig. 11).

In Fig. 12 we present the united profile from all wires. Profile widening, especially at the tails, takes place as a result of coefficient determination inaccuracy from equation (4).

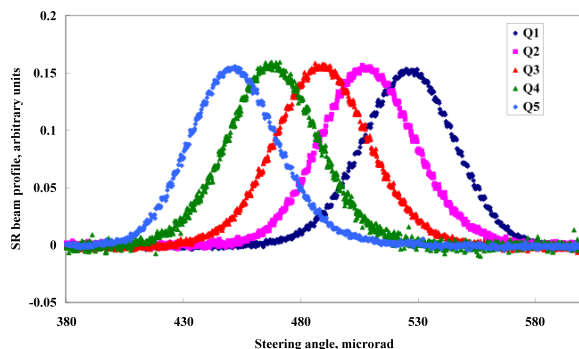


Fig. 11: Recovered profiles from separate wires.

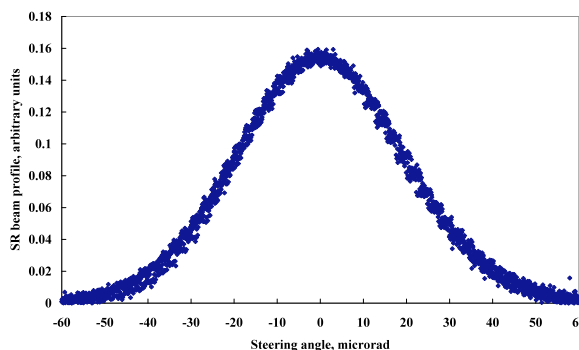


Fig. 12: Synchrotron radiation beam profile recovered from all wires.

## DISCUSSION

As we mentioned above the vibrating wire sensors can be used for many types of beam diagnostics because only a small amount of heat transfer from the measured object to wire is needed. Therefore vibrating wire sensors can be successfully applied to electron, proton, ion and photon beam monitoring. It is very important that in each of mentioned areas, due to its extreme sensitivity, VWS can perform measurements that are impossible using any other existing technologies. For charged particle beam diagnostics, its can make weak beam measurements and provide beam halo and tails monitoring. For photon beams it is possibility to measure very hard spectral components. Because of this one can measure only necessary part of radiation from insertion devices and cut unwanted contributions from other accelerator sources.

A possible area of VWS application is neutral beam diagnostics (neutrons, ion beams with uncompensated positive and negative charged particles, plasma). Recent application of the VWS in air has allowed a dramatic reduction in response time, together with a reduction in system cost by a large factor. The VWS concept shows a lot of promise due to its very high sensitivity and overall simplicity in both the mechanical design and electronics.

## ACKNOWLEDGMENTS

The author is grateful to all his co-authors with whom he worked many years. Many thanks to the YerPhI, PETRA and APS ANL staff for their friendly help during the experiments. Special thanks to R. Reetz and J. Bergoz for permanent interest and essential support.

## REFERENCES

1. McKenna G.T., Grouted-in installation of piezometers in boreholes. *Geotechnical J.*, 1995, 32, pp. 355-363.
2. Agejkin D.I. et al., in *Control and Regulation Pickups*, Moscow, 1965.
3. Asch G., *Les capteurs en instrumentation industrielle*, 1991.
4. T. Simmonds, Vibrating wire tiltmeters and inclinometers, recent developments and experiences. - *Monosys Guide in Monitoring*, 2000, Q-3, pp. 6-8.
5. Bourquin F., Joly M., A magnet-based vibrating wire sensor: design and simulation. *Smart Mater. Struct.* 14 (2005), 247-256.
6. Correia da Mata J.L.G., Fareleria J.M.N.A., Oliveria C.M.B.P., Wakeham W.A. A new instrument to perform simultaneous measurements of density and viscosity of fluids using a dual vibrating-wire technique. [www.zae-bayern.de/ectp/abstracts/correia\\_da\\_mata1.html](http://www.zae-bayern.de/ectp/abstracts/correia_da_mata1.html).
7. Krause A., Erbe A., Blick R.H. Nanomechanical vibrating wire resonator for phone spectroscopy in liquid helium. *Nanotechnology*, 2000, 11, pp. 165-168.
8. Temnykh A., The use of vibrating wire technique for precise positioning of CESR fase III super-conducting quadrupoles at room temperature. *Proc. of the 2001 Part. Accel. Conf. (Chicago, 2001)*, pp. 3469-3471.
9. Temnych A., Vibrating wire field-measuring technique. *Cornell CBN 96-7*, 1996.
10. Temnych A., The magnetic center finding using vibrating wire technique. *CBN 99-22*, 1999.
11. Ayazi F., Najafi K., A HARPSS polysilicon vibrating ring gyroscope.- *J. of Micromechanical Systems*, 2001, 10, 2, pp. 169-179.
12. Arutunian S.G., Mailian M.R., Wittenburg Kay, *Nucl. Instrum. Methods A*, 572, 1022-1032 (2007).
13. Elcev Ju.F., Zakosarenko V.M., Tsebro V.I. String magnetometer.- *Transition processes in superconducting magnetic systems*, Trudy FIAN, v. 150, Moscow, pp. 141-147.
14. *Fundamentals of Quartz Oscillators*, Application Note 200-2, Hewlett Packard, Electronic Counters Series.
15. Arutunian S.G., Dobrovolski N.M., Mailian M.R., Sinenko I.G., Vasiniuk I.E. Vibrating wire for beam profile scanning. - *Phys. Rev. Special Topics.- Accelerators and Beams*, 1999, v. 2, 122801.
16. Abdelghani Zniber A., Dane Quinn D. Resonance capture in a damped three-degree-of-freedom system: Experimental and analytical comparison. *Int. J. of Non-Linear Mechanics*, 2006, 41, 10, pp. 1128-1142
17. <http://www.aoe.vt.edu/~simpson/aoe4154/hotwirelab.pdf>
18. Cooper R. et al. A program for neutron detector research and development. Oak Ridge National Laboratory, March 2003.
19. Arutunian S.G., Dobrovolski N.M., Mailian M.R., Vasiniuk I.E., Vibrating wire scanner: first experimental results on the injector beam of Yerevan synchrotron. *Phys. Rev. Special Topics, Accelerators and Beams*, 2003, v. 6, 042801.
20. Arutunian S.G., Avetisyan A.E., Dobrovolski N.M., Mailian M.R., Vasiniuk I.E., Wittenburg K., Reetz R., Problems of Installation of Vibrating Wire Scanners into Accelerator Vacuum Chamber. *Proc. 8th Europ. Part. Accel. Conf. (3-7 June 2002, Paris, France)*, pp. 1837-1839.
21. Arutunian S.G., Werner M., Wittenburg K. Beam tail measurements by wire scanners at DESY.- *ICFA Advanced Beam Dynamic Workshop: Beam Halo Dynamics, Diagnostics, and Collimation (HALO'03) (in conjunction with 3rd Workshop on Beam-beam Interaction) (May 19-23, 2003 Gurney's Inn, Montauk, N.Y. USA)*.
22. Arutunian S.G., Bakshetyan K.G., Dobrovolski N.M., Mayilyan M.R., Oganessian V.A., Soghoyan A.E., Vasiniuk I.E., Wittenburg K., Vibrating wire scanner parameters optimization. *Proc. 9th Europ. Part. Accel. Conf. (5-9 July 2004, Lucerne, Switzerland)*, pp. 2457-2459.
23. Arutunian S.G., Bakshetyan K.G., Dobrovolski N.M., Mayilyan M.R., Oganessian V.A., Soghoyan A.E., Vasiniuk I.E., Wittenburg K., Vibrating wire scanner parameters optimization. *Proc. 9th Europ. Part. Accel. Conf. (5-9 July 2004, Lucerne, Switzerland)*, pp. 2457-2459.
24. Aginian M.A., Arutunian S.G., Hovhannisyan V.A., Mailian M.R., Wittenburg K., Vibrating wire scanner/monitor for photon beams with wide range of spectrum and intensity. *NATO Advanced Research Workshop "Advanced Photon Sources and Their Application" (Nor Amberd, Armenia, August 29 - September 02, 2004)*.
25. Arutunian S.G., Dobrovolski N.M., Mailian M.R., Oganessian V.A., Vasiniuk I.E. Nonselective receiver of laser radiation on the basis of vibrating wire. *Proc. Laser 2000 (November 2000, Ashtarak, Armenia)*.
26. Aginian M.A., Arutunian S.G., Hovhannisyan V.A., Mailian M.R., Wittenburg K., Vibrating wire scanner/monitor for photon beams with wide range of spectrum and intensity. *NATO Advanced Research Workshop "Advanced Photon Sources and Their Application" (Nor Amberd, Armenia, August 29 - September 02, 2004)*.
27. Aginian M.A., Arutunian S.G., Mailian M.R., Vibration wire monitor for photon beams diagnostics: preliminary tests on laser beams. - *NATO Advanced Research Workshop, CANDLE (17-21 July, 2006,*

Yerevan, Armenia), "Brilliant Light Facilities and Research in Life and Material Sciences".

28. Decker G., Arutunian S., Mailian M., Rosenbaum G., First vibrating wire monitor measurements of a hard x-ray undulator beam at the Advanced Photon Source. DIPAC 2007.
29. B.K. Scheidt, DIPAC '05, Lyon, France (2005).
30. Decker G., Arutunian S., Mailian M., Vasiniuk I., these Proceedings.